

Index

- aerosol 220, 230
- ALD, *see* atomic layer deposition
- amide groups 128–129
- APCVD, *see* atmospheric pressure chemical vapor deposition
- APCVD reactor 239, 241–243, 245
- APCVD system 218, 222, 224, 226, 236
- argon 11, 218, 282, 285
- atmospheric pressure 218, 237, 275, 290, 333
- atmospheric pressure chemical vapor deposition (APCVD) 218, 221, 226, 229, 232–234, 236, 240
- atomic configurations 48–49, 54
- atomic layer deposition (ALD) 144, 221, 230–232, 235, 365
- atomic substitution 36, 38–39, 54

- bandgap 9, 19, 23, 35, 37–39, 41, 43, 50
- band structures 9, 41, 46, 373–374
- boundary conditions 237, 239, 244
- buffer layer 289, 300, 379

- carrier concentration 44–45, 47, 83
- carrier gas flow rate 228–229

- CFD, *see* computational fluid dynamics
- chemical phenomena 237
- chemical vapor deposition (CVD) 10, 36, 75, 82, 144, 198, 215–236, 238, 240, 242, 244, 246, 328, 365, 383–384
- CHFS, *see* continuous hydrothermal flow synthesis
- climate change 2
- composite films 73, 85, 148, 158, 161–163, 166, 194, 201–202, 205, 353–354, 377–378, 389
- composite structures 273, 376–378, 388
- 3D-printed 378
- computational fluid dynamics (CFD) 236, 242
- continuous hydrothermal flow synthesis (CHFS) 204
- crystal structure 5, 10, 49–50, 112, 183, 186, 300, 305, 374
- double-layered 183–184
- CVD, *see* chemical vapor deposition
- CVD process 216–218, 237
- CVD techniques 218, 220–221, 232, 236

- DCMS, *see* direct current magnetron sputtering
- density functional theories (DFT) 40, 43
- DFT, *see* density functional theories

- dielectric constants 64, 66–67
- direct current magnetron sputtering (DCMS) 283, 285, 294, 299
- DMFT, *see* dynamic mean-field theory
- dopants 17, 35–36, 46–47, 49, 54, 306, 347–349, 376
- double clear glass 388–389
- dual-phase transformation 124–125, 131, 134, 149, 155
- dynamic mean-field theory (DMFT) 43, 45, 54

- EBD, *see* electron beam deposition
- electrical properties 184, 278
- electrical resistance changes (ERCs) 255–256, 269
- electron beam 274–275
- electron beam deposition (EBD) 275–279
- electronic structures 38, 42, 44, 47–48, 50, 54, 342
- energy 7, 35, 47–48, 52, 82–83, 90, 139, 202–203, 236–237, 239–240, 244, 252, 259, 265, 272–273
 - free 240
 - kinetic 219, 282
- energy conservation abilities 389
- energy consumption 373, 387, 389–390
- energy-efficient windows 180, 182, 184, 186, 188, 190, 192, 194, 196, 198, 200, 202, 204, 386
- epitaxial growth 255–256, 269, 299
- ERCs, *see* electrical resistance changes
- excellent thermochromic properties 201, 204

- fatigue life time, efficient 366
- FDTD, *see* finite-difference time-domain
- Fermi level 37–38, 40, 50
- film deposition techniques 215, 217
- film growth 222, 224, 227, 300–301
- film preparation, thin 252–253, 270, 280
- films 14, 17–18, 73–74, 131–132, 201–202, 216–217, 220–223, 227–228, 254–256, 275, 277–280, 300–301, 306–307, 336, 386
 - annealed 278
 - as-deposited 275, 277
 - composite thin 21, 108, 162
 - crystalline 220, 222
 - flat 377–378
 - flexible 190–191, 198, 353
 - intermediate 102, 246
 - sample 111
 - thin 9–11, 16–18, 71–74, 101–103, 109–110, 112–113, 124–126, 133–134, 219–222, 253, 255–256, 269–272, 278–284, 286–292, 294–299
- finite-difference time-domain (FDTD) 91, 142, 146, 154
- float glass 10–11, 383
 - blank 84, 164
- flow rate 218, 223–225, 228, 236, 244
 - total 222–224, 232
- flow ratios 287–290, 292, 295
- fluid 181, 236–239, 243–244, 246
- freeze-drying 124, 131, 133–134

- gels 9, 328–329, 332, 355
 - vanadium-oxane polymer 332
- geometry 41, 217, 219, 239, 242, 245

- glass 11, 101, 105, 160, 192, 198, 201, 262, 268, 305–306, 308–310, 313, 377, 379, 388–389
 - smart 309–310
 - soda-lime 289
- glass slides 160
- glass substrate 103, 141–142, 157, 241–242, 245–246, 299, 303, 311, 329, 347, 376
- glass surface 310
- grain size 256, 335–336
- grid structures 144–149, 151, 153, 155
- growth 38, 77, 150, 179, 181, 189, 196, 222, 226, 270, 300
 - heteroepitaxial 301–302
- growth temperature 222, 224–225, 231
- growth window 222–225, 228

- HAADF, *see* high-angle annular dark field
- heat transfer 243–244
- high-angle annular dark field (HAADF) 194–195
- hydrate precursor 195–196
- hydrogels 155–156
- hydrolysis 328–329, 332, 338–339, 355
- hydrothermal method
 - microwave-assisted 202–203
 - one-step 77, 188–189, 191
- hydrothermal synthesis 180–183, 191, 199, 204–205
- hydrothermal technology 180
- hysteresis width 194, 197, 339, 347–348

- ICMS, *see* inverted cylindrical magnetron sputtering
- incident light 87, 101, 142–143, 145, 167, 188, 377–378
- indium tin oxide (ITO) 11, 105, 168, 192, 225, 297, 300, 312
- inorganic precursors 222, 332
- inorganic thermochromic materials 3, 5
- inverted cylindrical magnetron sputtering (ICMS) 297
- ITO, *see* indium tin oxide

- kirigami structure 385, 387

- laser 252, 257–267, 274
- lattice 38–39, 47, 82, 269
- layers 7, 18–19, 80, 91, 106–107, 145, 168, 245, 303, 312, 365
 - seed 201, 285, 299–304
- LCs, *see* liquid crystals
- LCST, *see* lower critical solution temperature
- LDA, *see* local density approximation
- LGLs, *see* light guide layer
- lifetime 308
- light guide layer (LGLs) 91, 167
- light scattering effects 69, 167
- liquid crystals (LCs) 155, 160–161
- local density approximation (LDA) 43, 45, 54
- localized surface plasmon resonance (LSPR) 144, 153–154, 387
- lower critical solution temperature (LCST) 87, 154, 156
- low-temperature deposition 282, 290
- LSPR, *see* localized surface plasmon resonance
 - active 387

- magnesium 16, 18, 23, 35, 260, 266
- magnetron 116, 202–203, 301
- magnetron sputtering (MS) 10, 71, 73–74, 81–82, 283, 285, 294, 303, 328, 365
- MBE, *see* molecular beam epitaxy
- MCC, *see* monolayer colloidal crystal
- metal-insulator transition 255
- metal-organic chemical vapor deposition (MOCVD) 218–219, 226, 232, 234
- metastable phase 183, 191, 195
- microstructures 67, 187, 283, 287, 290, 302
- MOCVD, *see* metal-organic chemical vapor deposition
- molecular beam epitaxy (MBE) 170, 279–282
- monoclinic, low-temperature 8–9
- monolayer colloidal crystal (MCC) 125, 151
- MS, *see* magnetron sputtering
- multilayer film 81, 309–310
- multilayer structures 17, 63, 151, 166, 310, 313

- nanodome arrays 113, 126, 128, 151–153
- nanoparticle arrays 113, 128, 153
- nanopores 73–74
- nanosheets 182, 194, 196–197
- nanospheres 20, 151–153

- optical constants 66, 71–72, 74, 125, 134, 145
- optical performance 22, 66–67, 69, 71–72, 74, 77, 80, 82–83, 92, 124, 127, 131, 151, 352
 - better 74–76
- optical properties 5, 8, 48, 51–52, 54, 71, 74, 77, 80, 160–161, 292, 295, 309, 311, 343–344
- optical transmittance 193, 201–202, 307
- organic precursors 222, 332, 338–339, 355
- oxygen flow rate 225–227
- oxygen flow ratio 284–285, 287
- oxygen pressures 228, 254

- PAD, *see* polymer-assisted deposition
- PE, *see* plasma etching
- phase transition temperature 77, 83, 105, 124, 193, 197, 269, 300, 341–342, 344, 346
- photonic crystals 143
- physical properties 43, 45, 139
 - basic 43–44
- physical vapor deposition (PVD) 251–252, 254, 256, 258, 260, 262, 264, 266, 268, 270, 272, 274, 276, 282, 383–384
- plasma 219–220, 227, 234, 274, 282, 285, 294, 298
- plasma etching (PE) 126, 152
- PLD, *see* pulsed laser deposition
- polymer-assisted deposition (PAD) 81, 111, 124–125, 128, 134, 328
- polymers 7, 9, 20, 128–130, 217, 355, 376
- porous design 124–125, 134
- porous structures 124, 130–131, 287, 344
- precursor materials 181–182
- preparation process 75–76, 81, 85, 92
- primitive unit cells 47
- protective layers 163, 365

- pulsed laser deposition (PLD) 82, 198, 252–253, 256, 269–270, 277–279, 281
- PVD, *see* physical vapor deposition
- quartz 91, 103, 256–257, 259, 261, 263, 265, 267, 334
- glass 85, 103–104, 292
- substrate 149, 201, 350
- tube 241–244
- rapid thermal annealing (RTA) 333
- reactive pulse laser deposition (RPLD) 252–253, 255, 257, 259, 261, 263, 265, 267, 269
- reduction process, valence 333
- resistance 269–271, 334
- resistance change 275, 278, 280–281, 334
- room temperature 1, 5–6, 16, 23, 36–37, 39, 156, 158, 191, 197, 280, 289–290, 299, 341, 346
- RPLD, *see* reactive pulse laser deposition
- RTA, *see* rapid thermal annealing
- rutile phases 342, 369
- sapphire 150, 257–268, 271, 299, 301, 303
- sapphire substrates 150, 199, 225, 254, 256
- SCs, *see* solar cells
- shell materials 363, 365
- silica substrates 344, 346, 348
- fused 131, 133, 142
- silicon 220, 256, 258, 261, 263, 267, 293
- smart films/coatings 383
- smart windows 64, 84–86, 88–90, 92, 142–144, 160, 165, 167–170, 197–198, 205, 303–305, 308–310, 373–375, 380–381, 383–386
- applications 87, 156, 158–159, 273, 304
- composite 389
- energy-efficient 204–205
- works 114, 145
- solar cells (SCs) 82, 90–92, 105, 165, 167–168, 198
- solar energy 1, 3, 80, 82–83, 87, 90–93, 190
- utilization of 87, 93
- solar energy modulation
- ability 64, 72–73, 80–81, 143, 272
- solar modulation 104–105, 108–112, 119, 142, 144–145, 304, 308, 377–378
- solar modulation ability 113, 355, 362, 368, 375–377
- solar radiation 307, 361, 376, 378
- sol-gel method 108, 328–329, 332, 339, 342, 347–348, 351–352, 355–356
- organic 328, 338, 350
- solution methods 73, 75, 85, 104, 109, 363
- source material 282, 298
- square hole lengths 146–147
- square lattices 146–147
- structural phase transition 44, 196
- substrate 11, 102–103, 216–217, 220–221, 225–226, 231, 244–245, 252–253, 255, 269, 271–283, 286–293, 295–299, 301, 328–329
- bias 284–285, 294–295
- fluorine-doped-tin-oxide-precoated
- borosilicate 222
- materials 270, 293

- substrate surface 103, 216–217, 231, 298
- substrate temperature 223, 255, 283–288, 290, 293, 295, 300
 - high 284
 - higher 255, 293
 - low 255, 289, 302, 311–312
- supercell 47–48, 186
 - structure 112
- target materials 294, 298
- temperature change 3, 158, 309–310
- temperature-dependence
 - resistance 271
- temperature range 224–225, 228, 269, 333
- template-free methods 127, 149, 151, 155
- templates 112–113, 151, 153
- tetragonal, high-temperature 8–9
- theoretical simulations 36, 53–54, 69, 71, 75
- thermochromic 3–4, 7–8, 156, 165, 169, 192–193, 310–311, 339, 342–344, 363, 374, 380, 385, 389
- thermochromic films 198, 301, 307, 363, 366
 - flexible 165
- thermochromic hydrogels 156
- thermochromic materials 3, 5, 7
- thermochromic performance
 - 35–36, 38, 40, 42, 44, 46, 48, 50, 52–54, 123–125, 144, 146–148, 188, 362–363, 366
- thermochromic properties 1, 102–105, 123, 125, 155, 161–162, 190–191, 198–199, 201, 203–204, 336–337, 342, 344, 351–352, 355
- transition temperature 40, 48, 221, 256, 292–294, 304, 307, 336–337, 341–342, 344, 346–348, 375, 390
 - critical 346–347
 - critical phase 347, 355
 - reduced phase 109, 190
- transmission spectra 293, 295–296, 346
- transmittance 12, 15, 17–20, 69, 71–72, 106, 112–114, 161–163, 170, 202–204, 305–307, 335–336, 339–343, 346–347, 366–367
- changes 87, 158, 344
- hysteresis loop 169–170, 340
- simulated spectra 72
- temperature-dependent 195, 348–349
- valleys 144, 153
- transparent conductive films 169
- transparent materials 20, 165
- vanadium 8–9, 222, 230, 257–259, 261–265, 267–268, 272, 276, 280–281, 285, 287, 298, 306, 380–381, 383
 - oxidation of 290
 - alkoxides 332, 338, 355
- vanadium dioxide 1, 3, 5, 23, 123–124, 181, 284, 361, 373, 379
- vanadium films 299
- vanadium metal 298, 300
- vanadium oxide films 276, 290–291
- vanadium oxides 229, 252–253, 287, 291, 306, 332, 362, 380
- vanadium source 126, 189, 221, 223–224
- vanadium target 256, 276
- visible light 1, 3–4, 53, 89, 92–93, 127, 142, 158, 307, 341, 376–377

visible light transmittance 1, 113,
201, 307, 344, 347, 350,
355–356, 376

visible transmittance 37, 39, 131,
134, 199, 230, 340–341, 346,
387

wavelength range 6, 16, 21,
343–344

wintertime 376–378

X-ray diffraction (XRD) 84, 271,
277, 287, 293, 301, 333,
363

XRD, *see* X-ray diffraction

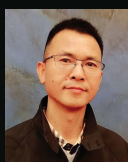
XRD patterns 254, 290–293, 300,
302, 364

XRD spectra 287–288, 291, 297

The usage of building energy accounts for 30–40% of total energy consumption in developed countries, exceeding the amount for industry or transportation. Around 50% of energy for building services is contributed by heating, ventilation, and air-conditioning (HVAC) systems. More importantly, both building and HVAC energy consumption are predicted to increase in the next two decades. Windows are considered as the least energy-efficient components of buildings. Therefore, smart windows are becoming increasingly important as they are capable of reducing HVAC energy usage by turning transmitted sunlight in a smart and favoured way: blocking solar irradiation on hot days, while letting it pass through on cold days. Compared with other types of smart windows, thermochromic windows have the unique advantages of cost-effectiveness, rational stimulus, and passive response. This book covers fabrication of vanadium dioxide-based smart windows, discusses various strategies to enhance their performance, and shares perspectives from top scientists in this particular field. It is the first book dedicated to this specific area that can well serve as a textbook for young researchers interested in solving the biggest problems of window energy consumption and, more importantly, inspire fresh ideas in and facilitate the commercialization of this particular technology.



Yi Long is a senior lecturer in the School of Materials Science and Engineering at Nanyang Technological University, Singapore. She obtained her PhD from the University of Cambridge, UK. Her research focuses on nanostructured functional materials for different applications. She has successfully implemented technology transfer from lab to industry for hard-disk companies in her early career. Her recent research is focused on developing various functional materials by manipulation of structure at the nanoscale to achieve unusual properties and focus on energy-saving windows, flexible electronics, and smart devices. Her work has been widely highlighted in top journals and different media.



Yanfeng Gao is the group leader of light/thermal modulated materials at Shanghai University. From 2004 to 2012, he worked at the Shanghai Institute of Ceramics, Chinese Academy of Sciences, Musashi Institute of Technology, and Nagoya University. Dr. Gao has published over 190 journal papers and filed over 100 patents. He is a recipient of the prestigious Changjiang Scholar Award and the National Science Fund for Distinguished Young Scholars.



JENNY STANFORD
PUBLISHING

V768

ISBN 978-981-4877-06-0



9 789814 877060